Inorg. Chem. **2003**, *42*, 532–540

Electronic Structures and Nonlinear Optical Properties of Trinuclear Transition Metal Clusters M–(μ-S)–M′ (M = Mo, W; M′ = Cu, Ag, Au)

Xihua Chen,[†] Kechen Wu,*[,†] Jaap G. Snijders,[‡] and Chensheng Lin[†]

State Key Laboratory of Structural Chemistry, Fujian Institute of Research on the Structure of Matter, Chinese Academy of Sciences, Fuzhou, Fujian 350002, China, and Theoretical Chemistry Group, Materials Science Center, Groningen University, AG 4797 Groningen, The Netherlands

Received April 12, 2002

A series of trinuclear metal clusters $MS_4(M'PPh_3)_2(M'PPh_3)$ (M = Mo,W; M′ = Cu, Ag, Au) have been studied using the density functional theory (DFT) method. The static polarizabilities and hyperpolarizabilities of the model clusters have been calculated using the finite-field (F-F) method. The model clusters, divided into two groups, are alike in the structure of two fragments of rhombic units M–(μ-S)$_2$–M′ (M = Mo, W; M′ = Cu, Ag, Au), perpendicular to each other, which are joined by sharing the bridge metal M. It is the charge transfer from one of these moieties to the other in these characteristic sulfido–transitional metal cores that is responsible for the polarizabilities and hyperpolarizabilities. This kind of electronic delocalization, different from that of the planar π-system, is interesting and warrants further investigation. The structural effects on properties are important. In these models, considerable third-order nonlinearities are exhibited. The element substitution effect of Mo and W is weak, while that of Cu and Ag is relatively substantial. An overall order is γ_{xxxx}(Mo–Ag) > γ_{xxxx}(W–Ag) > γ_{xxxx}(Mo–Au) > γ_{xxxx}(W–Au) > γ_{xxxx}(Mo–Cu) > γ_{xxxx}(W–Cu) and γ_{av}(Mo–Ag) ∼ γ_{av}(W–Ag) > γ_{av}(Mo–Au) ∼ γ_{av}(W–Au) ∼ γ_{av}(Mo–Cu) ∼ γ_{av}(W–Cu).

Having been rapidly developed over the last four decades, novel nonlinear optical (NLO) materials are still in great demand due to the critical role that they are playing in contemporary photonics devices.[1] Some excellent inorganic mineral oxide NLO materials including KH_2PO_4 (KDP),[2] $LiNbO_3$,[3] β-BaB_2O_4 (BBO),[4] and LiB_3O_5 (LBO)[5] have already been successfully commercialized. During the past two decades, efforts have been extensively devoted to the studies of semiconductors, conjugated polymers, and organic crystals.[1,6] In recent years, much attention has also been paid to fullerenes,[7] Schiff-base metal complexes,[8] and other organometallic compounds.[9] Inorganic metal cluster compounds, on the other hand, seem to have been largely overlooked until recently.[10] In fact, transition-metal clusters offer a large variety of structures and a diversity of electronic properties shaped by the metal-characterized core. They may comprise a promising family of NLO materials, besides their special roles demonstrated in catalytic reactions,[11] biological chemical processes,[12] and magnetic materials.[13] It is believed that metal clusters may possess the combined advantages of both organic polymers and inorganic semiconductors.

Among the most typical transition-metal cluster compounds, M−(μ-S)$_2$−M′ species (M = Mo, W; M′ = Cu. Ag,

* To whom correspondence should be addressed. E-mail: wkc@ms.fjirsm.ac.cn. Fax: +86-591-3714946.

[†] Fujian Institute of Research on the Structure of Matter.

[‡] Groningen University.

(1) Karna, S. P. *J. Phys. Chem. A* **2000**, *A104*, 4671.
(2) Smith, W. L. O. *Appl. Opt.* **1977**, *16*, 798.
(3) Boyd, G. D.; Miller, R.C.; Nassau, K.; Bond, W. L.; Savage, A. *Appl. Phys. Lett.* **1964**, *16*, 1856.
(4) Chen, C.; Wu, B.; Jiang, A.; You, G. *Sci. Sin., Ser. B* **1985**, 235.
(5) Chen, C.; Wu, Y.; Jiang, A.; Wu, B.; You, G.; Li, R.; Lin, S. *J. Opt. Soc. Am.* **1989**, *B6*, 616.
(6) Williams, D. J., Ed. *Nonlinear Optical Properties of Organic and Polymeric Materials*; ACS Symposium Series 233; American Chemical Society: Washington, DC, 1983.
(7) (a) Tutt, L. W.; Kost, A. *Nature* **1992**, *356*, 225. (b) Mclean, D. G.; Sutherland, R. L.; Brant, M. C.; Brandelik, D. M.; Fleitz, P. A.; Pottenger, T. *Opt. Lett.* **1993**, *18*, 858.
(8) Averseng, F.; Lacroix, P. G.; Malfant, I.; Dahan, F.; Nakatani, K. *J. Mater. Chem.* **2000**, *10*, 1013.
(9) (a) Mtsuzawa, N.; Seto, J.; Dixon, D. A. *J. Phys. Chem.* **1997**, *A101*, 9391. (b) Whittall, I. R.; Mcdonagh, A. M.; Humphrey, M. G.; Samoc, M. *Adv. Organomet. Chem.* **1998**, *42*, 291.
(10) Shi, S. Nonlinear Optical Properties of Inorganic Clusters. In *Optoelectronics Properties of Inorganic Compounds*; Roundhill, D. M., Fackler, J. P., Jr., Eds.; Plenum Press: New York, 1998; Chapter 3 and the references therein.
(11) Bose, A.; Saha, C. R. *J. Mol. Catal.* **1989**, *49*, 271.
(12) Mclendon, G.; Martell, A. E. *Coord. Chem. Rev.* **1976**, *19*, 1.
(13) Gatteschi, D.; O. Kahn, O.; Miller, J. S.; F. Palacio, F. *Magnetic Molecular Materials*; Reidel: Dordrecht, The Netherlands, 1991.

10.1021/ic025649e CCC: $25.00
Published on Web 12/17/2002

Table 1. Crystal Data of Six Trinuclear Transition Metal Cluster Compounds (a) $MoS_4Cu(PPh_3)_2Cu(PPh_3)$, (b) $MoS_4Ag(PPh_3)_2Ag(PPh_3)$, (c) $WS_4Cu(PPh_3)_2Cu(PPh_3)$, (d) $WS_4Ag(PPh_3)_2Ag(PPh_3$, (e) $MoS_4Au(PPh_3)Au(PPh_3)$, and (f) $WS_4Au(PPh_3)Au(PPh_3)$

param	a	b	c	d	e	f
cryst system	monoclinic	monoclinic	monoclinic	monoclinic	triclinic	triclinic
space group	$P2_1/c$	$P2_1/c$	$P2_1/c$	$P2_1/c$	$P\bar{1}$	$P\bar{1}$
a (Å)	18.394(4)	18.154(4)	18.372(6)	18.111(2)	9.596(1)	9.545(2)
b (Å)	16.653(3)	17.322(3)	16.702(7)	17.356(2)	10.630(1)	10.590(2)
c (Å)	17.714(3)	17.790(3)	17.740(8)	17.797(2)	19.712(2)	19.674(3)
α (deg)	90.0	90.0	90.0	90.0	89.06(1)	89.07(2)
β (deg)	95.53(1)	95.11(2)	95.56(3)	95.02(1)	80.87(1)	80.86(2)
γ (deg)	90.0	90.0	90.0	90.0	66.99(1)	67.36(2)

Au) have been widely studied and reviewed.[14−16] One of the most remarkable features of this cluster family is the regular building from the simplest mono-Mo(W)−mono-Cu(Ag, Au) clusters to the much larger ones, which may be composed of up to 20 metallic atoms, and the polymeric cluster complexes. The fruitful chemistry of Mo(W)−S−Cu(Ag, Au) clusters has demonstrated the great affinity between Cu/Ag/Au cations (strong soft acids) and thiomolybdate/thiotungstate anions (strong soft bases), which has led to a number of transitional metal cores for numerous and structurally novel multinuclear complexes.

Several papers have reported the experimental measurements of the NLO responses in the metal cluster family including optical absorption, self-focusing, refraction, and optical-limiting effects.[10,17−20] Some of the clusters show considerable third-order NLO responsibilities comparable to or even much stronger than those of C_{60}, which is one of the best molecules reported for optical limiting.[21,22] The NLO properties of clusters with three basic structural types, i.e., butterfly-, cubic cage-, and nest-shaped, were compared, and a qualitative structure−NLO property relationship was discussed.[21] The results of these experiments are greatly encouraging.

However, the traditional trial-and-error method is insufficient to achieve satisfactory progress in this field. Thorough investigations with powerful theoretical methods provide detailed understanding of the structure−property relationship and inspire the design and simulations of novel NLO materials at the molecular level. The information regarding the microscopic origins of the NLO responses of these clusters and what particular cluster cores or structure types contribute most to effective NLO properties is still needed. Since the prerequisite for large bulk NLO responses is that the constituent molecules have large molecular NLO responses, efforts should be directed toward understanding the structure−property relations of individual molecular clusters for further molecular engineering strategies.

In this paper, a series of typical trinuclear metal clusters Mo(W)−S−Cu(Ag, Au) are modeled and geometrically optimized. The static polarizabilities and hyperpolarizabilities of these simulating models are then calculated using the finite-field (F-F) method, and the results are compared and discussed. The electronic structures and external field perturbation effects on the molecules are analyzed, and discussions have been made trying to reveal the origin of the NLO properties of this family of cluster compounds.

Theoretical Methods

The calculation of the static polarizabilities and hyperpolarizabilities of a molecule is straightforward in a finite-field approach.[23−25] Suppose that an uncharged molecule is placed in weak homogeneous static electric fields. The energy can be expressed by the Buckingham type expansion:[26]

$$\Delta E(F_i,F_j,F_k) = E(F_i,F_j,F_k) - E_0 = -\mu_i F_i - (1/2)\alpha_{ij}F_iF_j - (1/6)\beta_{ijk}F_iF_jF_k - (1/24)\gamma_{ijkl}F_iF_jF_kF_l \quad (1)$$

Here E is the energy of the molecule under the electric field $\mathbf{F}$, E_0 is the unperturbed energy of the free molecule, F_i is the vector component of the electric field along the i direction, and μ_i, α_{ij}, β_{ijk}, and γ_{ijkl} are the dipole moment, linear polarizability, first-order hyperpolarizability, and second-order hyperpolarizability, respectively. In eq 1, each Greek subscript of $i-l$ denotes the indices of the Cartesian axes x, y, or z and a repeated subscript means a summation over its corresponding index.

The independent tensor components of μ_i, α_{ij}, β_{ijk}, and γ_{ijkl} of a specified molecule depend on its molecular symmetry. As the molecules concerned in this paper are all of C_1 symmetry, 3, 6, 10, and 15 independent components are needed to specify μ_i, α_{ij}, β_{ijk}, and γ_{ijkl}, respectively. Accordingly, a set of 34 appropriate energy differences, $\Delta E(F_i,F_j,F_k)$, are required to resolve these tensor components. The general formulation was published by Dupuis et al.,[27] and the general formulations for molecules with major molecular point group symmetries were also summarized in our previous paper.[28]

(14) Stiefel, E. I.; Matsumoto, K., Eds. *Transition Metal Sulfur Chemistry−Biological and Industrial Significance*; American Chemical Society: Washington, DC, 1996.
(15) Muller, A.; Diemann, E.; Jostes, R.; Bogge, H. *Angew. Chem., Int. Ed. Engl*. **1981**, *20*, 934.
(16) Sarkar, S.; Mishra, S. B. S. *Coord. Chem. Rev*. **1984**, *59*, 239.
(17) Hou, H. W.; Xin, X. Q.; Shi, S. *Coord. Chem. Rev*. **1996**, *153*, 25 and references therein.
(18) Shi, S.; Ji, W.; Xin, X. Q. *J. Phys. Chem*. **1995**, *99*, 894.
(19) Sankane, G.; Shibahara, T.; Hou, H. W.; Xin, X. Q.; Shi, S. *Inorg. Chem*. **1995**, *34*, 4785.
(20) Low, M. K.; Hou, H. W.; Zheng, H. G.; Wong, W. T.; Jin, G. X.; Xin, X. Q.; Ji, W. *Chem. Commun*. **1998**, 505.
(21) Shi, S.; Ji, W.; Lang, J. P.; Xin, X. Q. *J. Phys. Chem*. **1994**, *98*, 3570.
(22) Ajie, H.; Alvarez, M. M.; Anz, S. J.; Beck, R. D.; Diederich, F.; Fostiropoulos, K.; Hoffmann, D. R.; Kratschmer, W.; Rubin, Y.; Schriver, K. E.; Sensharma, D.; Wetten, R. L. *J. Phys. Chem*. **1990**, *94*, 8630.
(23) Cohen, H. D.; Roothaan, C. J. *J. Chem. Phys*. **1965**, *43*, S34.
(24) Perrin, E.; Prasad, P. N.; Mougenot, P.; Dupuis, M. *J. Chem. Phys*. **1989**, *91*, 4728.
(25) Kurtz, H. A.; Stewart, J. P.; Dieter, K. M. *J. Comput. Chem*. **1990**, *11*, 82−87.
(26) Buckingham, A. D. *Adv. Chem. Phys*. **1967**, *12*, 107.
(27) See the numerous works by M. Dupuis et al. For example: Sim, F.; Chin, S.; Dupuis, M.; Rice, J. E. *J. Phys. Chem*. **1992**, *97*, 1158−1163. Also: Maroulis, G. *J. Chem. Phys*. **1998**, *108*, 5432.
(28) Chen, X.; Lin, C.; Wu, K. *Chin. J. Struct. Chem*. **2001**, *20*, 369.

In a uniform approach, the explicit expressions for the diagonal tensor components, μ_i, α_{ii}, β_{iii}, γ_{iiii}, and γ_{iijj}, are

$$\mu_i = \frac{1}{2(\sigma - \sigma^3)F}\{\sigma^3[\Delta E(F_i) - \Delta E(-F_i)] - [\Delta E(\sigma F_i) - \Delta E(-\sigma F_i)]\}$$

$$= \frac{1}{2(\sigma - \sigma^3)F}\{[\sigma^3\Delta E(F_i) + \Delta E(-\sigma F_i)] - [\sigma^3\Delta E(-F_i) + \Delta E(\sigma F_i)]\} \quad (2)$$

$$\alpha_{ii} = \frac{1}{(\sigma^2 - \sigma^4)F^2}\{\sigma^4[\Delta E(F_i) + \Delta E(-F_i)] - [\Delta E(\sigma F_i) + \Delta E(\sigma F_i)]\} \quad (3)$$

$$\beta_{iii} = \frac{3}{(\sigma^3 - \sigma)F^3}\{\sigma[\Delta E(F_i) - \Delta E(-F_i)] - [\Delta E(\sigma F_i) - \Delta E(-\sigma F_i)]\}$$

$$= \frac{3}{(\sigma^3 - \sigma)F^3}\{[\sigma\Delta E(F_i) + \Delta E(-\sigma F_i)] - [\sigma\Delta E(-F_i) + \Delta E(\sigma F_i)]\} \quad (4)$$

$$\gamma_{iiii} = \frac{12}{(\sigma^4 - \sigma^2)F^4}\{\sigma^2[\Delta E(F_i) + \Delta E(-F_i)] - [\Delta E(\sigma F_i) + \Delta E(\sigma F_i)]\} \quad (5)$$

$$\gamma_{iijj} = \frac{1}{F^4}\{2[\Delta E(F_i) + \Delta E(-F_i) + \Delta E(F_j) + \Delta E(-F_j)] - [\Delta E(F_i,F_j) + \Delta E(-F_i,F_j) + \Delta E(F_i,-F_j) + \Delta E(-F_i,-F_j)]\} \quad (6)$$

where σF ($\sigma \neq 0, 1$) is a multiple of F. The suitable values of electric field strengths are crucial in finite-field computations.[29] We set median values so that F=0.0050 au and $\sigma F = 0.0030$ au with $\sigma = 0.6$.

The isotropic scalar values for μ, α, β, and γ averaged from their tensor components are defined as[30]

$$\alpha_{av} = \frac{1}{3}\sum_i \alpha_{ii} \quad i = x, y, z \quad (7)$$

$$\beta_{i,av} = \frac{1}{3}\sum_j \beta_{ijj} + \beta_{jij} + \beta_{jji} \quad i = x, y, z \quad (8)$$

$$\gamma_{av} = \frac{1}{5}\sum_{ij} \gamma_{iijj} \quad i = x, y, z \quad (9)$$

In this paper, six molecular clusters in the Mo(W)−S(Se)−Cu(Ag, Au) series have been modeled and studied. They include (a) $MoS_4Cu(PPh_3)_2Cu(PPh_3)$,[31] (b) $MoS_4Ag(PPh_3)_2Ag(PPh_3)$,[32] (c) $WS_4Cu(PPh_3)_2Cu(PPh_3)$,[32] (d) $WS_4Ag(PPh_3)_2Ag(PPh_3)$,[33] (e) $MoS_4Au(PPh_3)Au(PPh_3)$,[34] and (f) $WS_4Au(PPh_3)Au(PPh_3)$.[35]

A summary of the crystalline structure data of these clusters is given in Table 1. And the molecular structures of these clusters drawn from the measured data are shown in Figure 1. While the similarities of the crystal and molecular structures within this series are obvious, they can be categorized into two groups. Group 1 includes the isomorphous compounds a−d, while compounds e and f belong to group 2. Each of the crystals of group 1 is in monoclinic symmetry containing 4 molecules in a unit cell, which are in orientation nearly parallel with the *b* axis. Moreover, the cell parameters differ slightly from one to another, especially those of compounds a to c and b to d, which may indicate that the similarity between Mo and W is slightly more distinct than that between Cu and Ag. In group 1, two M′ (M′ = Cu, Ag) atoms are bridged by an essentially tetrahedral MS_4^{2-} (M = Mo, W) moiety, with one (M'_1) distortedly tetrahedrally coordinated and the other (M'_2) trigonally planar. On the other hand, the two crystals of group 2 have a triclinic unit cell, which is composed of two molecules. Though the crystal cell parameters of molecules e and f are again very close to each other, they are not at all comparable to those of group 1. In clusters e and f, the gold atoms have triangle geometry and the atoms P−Au−M(W)−Au−P form an approximately linear chain. Thus, the two Au atoms are nearly identical.

Groups 1 and 2 share a common feature in their geometric structures, namely, the three metal atoms in every molecule lie along a nearly straight line. Considering the practical computing economy, the above six prototype molecules were simplified by substituting the ligand PPh_3 with PH_3 and the simplified clusters were geometrically optimized. Thus, we obtain the model clusters, $MoS_4Cu(PH_3)_2Cu(PH_3)$ (**I**), $MoS_4Ag(PH_3)_2Ag(PH_3)$ (**II**), $WS_4Cu(PH_3)_2Cu(PH_3)$ (**III**), $WS_4Ag(PH_3)_2Ag(PH_3)$ (**IV**), $MoS_4Au(PH_3)Au(PH_3)$ (**V**), and $WS_4Au(PH_3)Au(PH_3)$ (**VI**) (Figure 2).

Although the simplification of the prototype clusters a−f is necessary with the consideration of the computing cost and efficiency, the phenyl group is thought to be more polarizable than hydrogen, which might result in the quantitative variations of the polarizability and hyperpolarizabilty of the clusters. However, as all model clusters were calculated at the same simplification level, the results would be sure to help us in understanding the relationship between the molecular structures and NLO property of these complexes.

In energy calculations, all six models were placed in such a coordinate system that the central Mo(W) atoms coincided with the original point. M'_1 (Cu_1 and Ag_1 of group 1, any of the two Au atoms of group 2) atoms were sited on the *x* axis along the positive direction. The rhombic moiety $M(\mu\text{-}S_1)(\mu\text{-}S_4)M'_1$ rested almost on the coordinate *xz* plane; another rhomboid of $M(\mu\text{-}S_2)(\mu\text{-}S_3)M'_2$ rested on the *xz* plane. The two P atoms in **V** and **VI** were located on the extension lines of Mo(W)−Au; in the molecules of group 1, P_3 was on the extension line of Mo(W)−Cu_2(Ag_2), while the delta P_1–Cu_1(Ag_1)−P_2 was near the *xy* plane (Figure 2). Throughout the energy calculations, the keyword "no symmetry" was used to maintain the orientation.

The proper theoretical methods and basis sets should be carefully selected to meet the requirements of both accuracy and computing economy. Density functional theory (DFT)[36,37] proved to be extremely useful in treating the electronic structures of molecules containing transitional metals.[38] Recently some reports presented

(29) Guan, J.; Duffy, P.; Carter, J. T.; Chong, D. P.; Casida, K. C.; Casida, M. E.; Wrinn, M. *J. Chem. Phys.* **1993**, *98*, 4753.
(30) Bishop, D. M. In *Advances in Chemical Physics*; Prigogime, I., Rice, S. A., Eds.; John Wiley & Sons: New York, 1998; Vol. 104.
(31) (a) Müller, A.; Bögge, H.; Tölle, H. G.; Jostes, R.; Schimanski, U.; Dartmann, M. *Angew. Chem., Int. Ed. Engl.* **1980**, *19*, 654. (b) Müller, A.; Bögge, H.; Schimanski, U. *Inorg. Chim. Acta* **1980**, *45*, L249.
(32) Müller, A.; Bögge, H.; Schimanski, U. *Inorg. Chim. Acta* **1983**, *69*, 5.
(33) Müller, A.; Bögge, H.; Koniger-Ahlborn, E. *Z. Naturforsch., B* **1979**, *34*, 1698.
(34) Charnock, J. M.; Bristow, S.; Nicholson, J. R.; Garner, C. D.; Clegg, W. *J. Chem. Soc., Dalton Trans.* **1987**, 303.
(35) Pritchard, R. G.; Moore, L. S.; Parish, R. V.; McAuliffe, C. A.; Beagley, B. *Acta Crystallogr., Sect. C* **1988**, *44*, 2022.
(36) Hohenberg, P.; Kohn, W. *Phys. Rev. B* **1964**, *136*, 864.
(37) Kohn, W.; Sham, L. J. *Phys. Rev. A* **1965**, *140*, 1133.

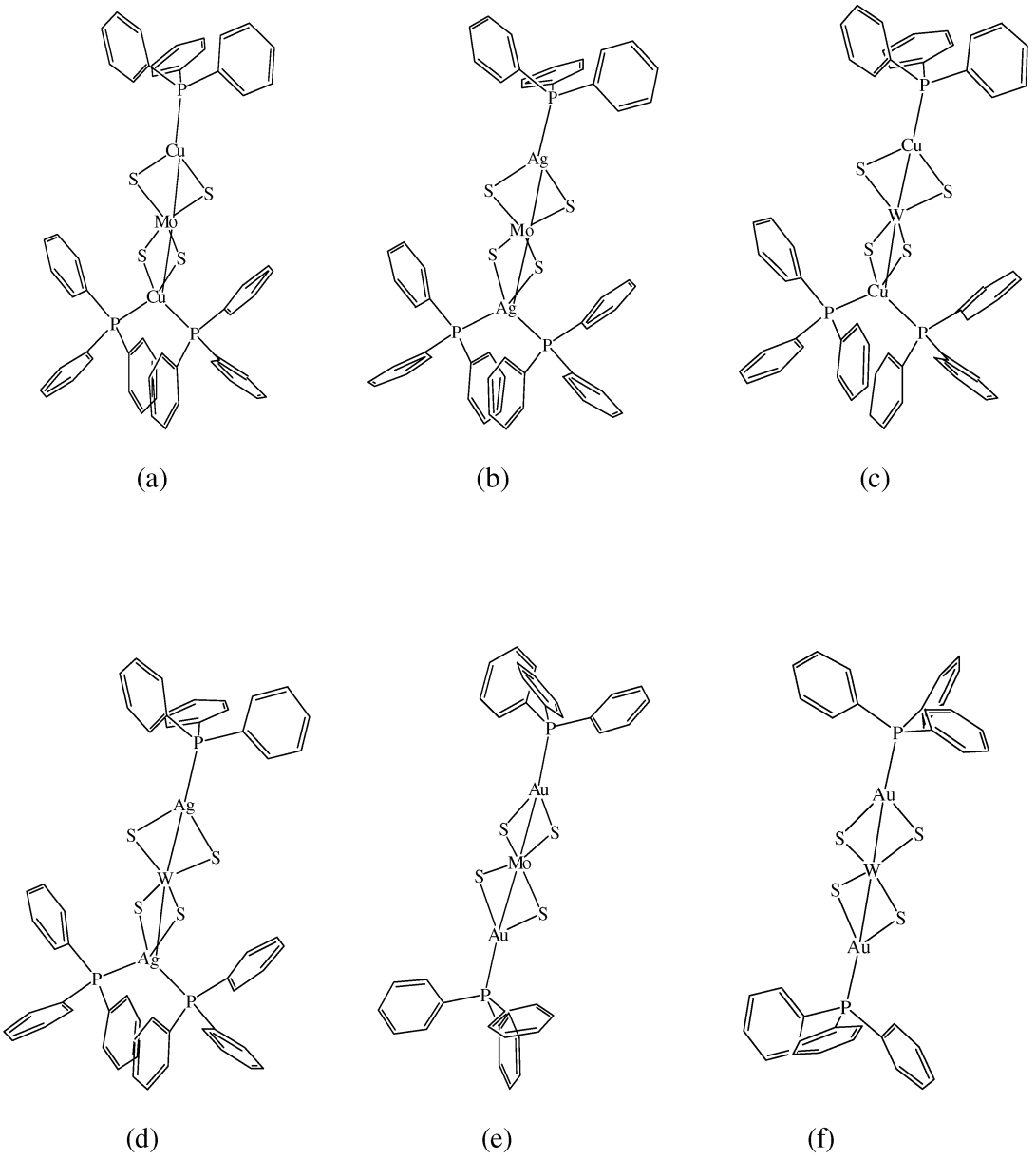

Figure 1. Structural depictions of clusters (a) $MoS_4Cu(PPh_3)_2Cu(PPh_3)$, (b) $MoS_4Ag(PPh_3)_2Ag(PPh_3)$ (c) $WS_4Cu(PPh_3)_2Cu(PPh_3)$, (d) $WS_4Ag(PPh_3)_2Ag(PPh_3)$, (e) $MoS_4Au(PPh_3)Au(PPh_3)$ and (f) $WS_4Au(PPh_3)Au(PPh_3)$.

the (hyper)polarizability of transition metal complexes with satisfactory results.[39] We adopted B3LYP with the gradient-corrected exchange potential of Becke and the gradient-corrected correlation potential of Lee, Yang, and Parr (BLYP). For all the atoms involved, the basis set LanL2DZ set applied, which means D95 on H atoms and Los Alamos ECP plus DZ on Mo, W, Cu, Ag, Au, S, Se, and P atoms. The density was converged to 10^{-6} for geometry optimizations and 10^{-8} for energy computations. A full set of 34 energy differences $\Delta E(F_i,F_j,F_k)$ was calculated, followed by the independent components μ_i, α_{ij}, β_{ijk}, and γ_{ijkl}. Special average values of α, β, and γ were computed on the basis of the finite-field approach. All geometric optimizations and energy calculations were carried out using the Gaussian 98 program package.[40]

It should be noted that some theoretical studies indicated the important influence of basis set on molecular optical (hyper)-polarizability and suggested polarization and diffuse functions be used in computation of conjugated organic molecules.[41,42] Since

(38) Sosa, C.; Andzelm, J.; Elkin, B. C.; Wimmer, E.; Dobbs, K. D.; Dixon, D. A. *J. Phys. Chem.* **1992**, *96*, 6630.
(39) For examples: (a) Ricciardi, G.; Rosa, A.; van Gisbergen, S. J. A.; Baerends, E. J. *J. Phys. Chem.* A **2000**, *104*, 635. (b) Lin, C.; Wu, K.; Snijders, J. G.; Sa, R.; Chen, X. *Acta Chim. Sin.* **2002**, *60*, 664.
(40) Gaussian 98, Revision A.7, Frisch, M. J.; Trucks, G. W.; Schlegel, H. B.; Scuseria, G. E.; Robb, M. A.; Cheeseman, J. R.; Zakrzewski, V. G.; Montgomery, J. A.;. Stratmann, R. E., Jr.; Burant, J. C.; Dapprich, S.; Millam, J. M.; Daniels, A. D.; Kudin, K. N.; Strain, M. C.; Farkas, O.; Tomasi, J.; Barone, V.; Cossi, M.; Cammi, R.; Mennucci, B.; Pomelli, C.; Adamo, C.; Clifford, S.; Ochterski, J.; Petersson, G. A.; Ayala, P. Y.; Cui, Q.; Morokuma, K.; Malick, D. K.; Rabuck, A. D.; Raghavachari, K.; Foresman, J. B.; Cioslowski, J.; Ortiz, J. V.; Stefanov, B. B.; Liu, G.; Liashenko, A.; Piskorz, P.; Komaromi, I.; Gomperts, R.; Martin, R. L.; Fox, D. J.; Keith, T.; Al-Laham, M. A.; Peng, C. Y.; Nanayakkara, A.; Gonzalez, C.; Challacombe, M.; Gill, P. M. W.; Johnson, B.; Chen, W.; Wong, M. W.; Andres, J. L.; Gonzalez, C.; Head-Gordon, M.; Replogle, E. S.; Pople, J. A. Gaussian, Inc., Pittsburgh, PA, 1998**.**
(41) Hurst, G. J. B.; Dupuis, M.; Clementi, E. *J. Chem. Phys.* **1988**, *89*, 385.
(42) Adant, C.; Brédas, J. L. *Nonlinear Opt.* **1994**, *8*, 87.

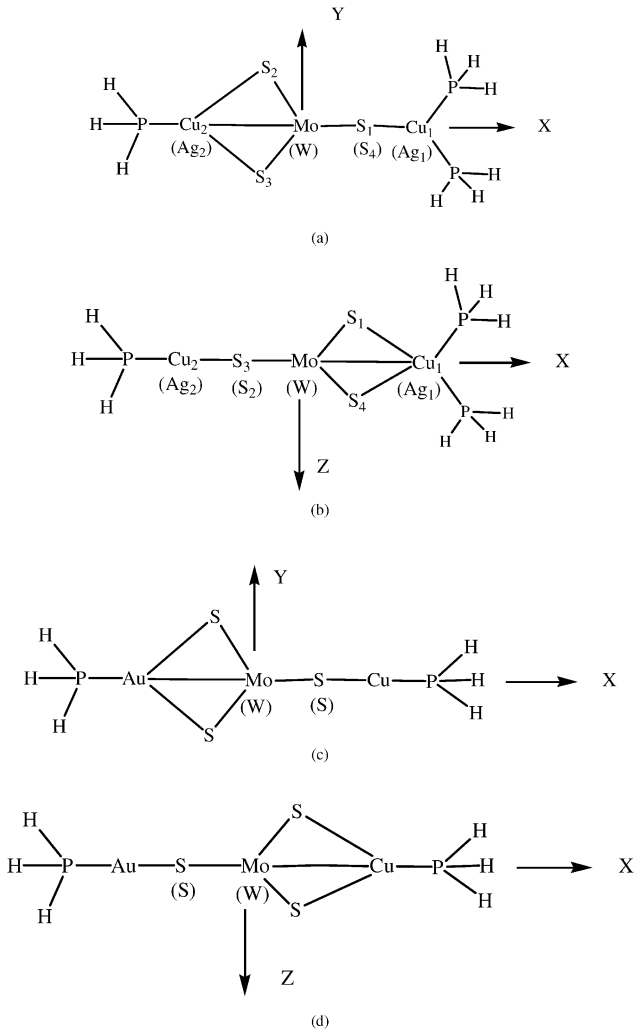

Figure 2. Molecular structures and orientations of model clusters (a) side view of group 1, (b) top view of group 1, (c) side view of group 2 and (d) top view of group 2.

no satisfactorily acceptable diffuses for all the heavy transition metal atoms involved in this paper are available, we adopted the basis set of LanL2DZ as a compromise between calculation quality and cost. The appropriate new basis with polarization and diffuse functions need to be developed and examined for these clusters.

Results and Discussion

Geometry Optimization. Model clusters **I**−**VI**, with all framework positional parameters inherited from their prototype compounds a−f, have been optimized at B3LYP/LanL2DZ level. Selected optimized bond lengths and angles are presented in Table 2. We found that no fundamental distortions were introduced by geometry optimizations for all five models. The shapes of the molecular frameworks remain without dissociation or general twist, and modifications of structural parameters occur within the reasonable error rate boundaries, where the largest bond changes (W−Ag_1 in molecule **IV**, +0.188 Å) average no more than 0.2 Å and smaller yet bond angle bascule motions are observed. The procedures of simplification and geometry optimization are very helpful to further costly property computations. In fact, the number of basis functions needed by the LanL2DZ basis set for the prototype molecule b, $MoS_4Ag(PPh_3)Ag(PPh_3)_2$, will reach 698, in contrast with only 140 for the simplified model **II**, $MoS_4Ag(PH_3)Ag(PH_3)_2$. However, some significant regularities and tendencies could be detected from the changes of the bond lengths and angles following the optimizations. These are as follows:

(1) In all species, the selected bonds were all stretched, and the degrees of extension occurred in similar orders. The unanimous increase of the M−M′ distance implies the interactions between these transitional metal atoms were weakened by substitution of the ligand PPh_3 with PH_3. This is not surprising. It is well-known that the PPh_3 ligand coordinating to M′ (Cu, Ag, Au) atoms is, although labile, an effective electron donor[43] and is therefore regularly used to stabilize metallic complexes. The metal−metal interactions are weak in Mo(W) transition metal clusters, and the stabilities of these compounds arises mainly from the bonding interactions between the metal atoms and the inorganic sulfur. Direct metal−metal electronic transfer is thus less important in this case, and the optimization results are acceptable. Increase of M−M′ distances are slightly different for M'_1 and M'_2 in molecules of group 1. For instance, in cluster **II**, $\Delta(Mo-Ag_1) = 0.173$ Å and $\Delta(Mo-Ag_2) = 0.136$ Å. The similar situation occurs in bonds of M′−P but with a reverse inequality: $\Delta(Ag_2-P)$ is slightly larger than $\Delta(Ag_1-P)$. Obviously, the different coordination numbers of the PPh_3 ligand on the two M′ atoms, as well as the different coordinating conditions of M'_1 and M'_2, are responsible. As one more PPh_3 combines with a tetrahedrally coordinated M'_2 atom, the effect of substitution by PH_3 doubles with $M-M'_2$ but is shared by M'_2−P bonds. On the other hand, for molecules of group 2, the bond lengths relating respectively to Au_1 and Au_2 tend to average, which is expected for the parity of the two trigonally coordinated Au atoms. Interestingly, increments of averaged M′−S bond lengths are much larger than those of M−S bonds. The shorter lengths and greater stability of M−S bonds are consistent with experimental data showing the affinity between Mo(W) and S is greater than that between Cu(Ag, Au) and S.

(2) During the optimizations, all models were altered in such a way that geometric regularity is considerably enhanced. In most species, the three metal atoms M'_1, M, and M'_2 tend to align in a straight pattern. At the same time, the bond angles of $M-S_1-M'_2$ and $M-S_4-M'_2$, as well as those of $M-S_2-M'_2$ and $M-S_3-M'_2$, tend to be respectively leveled due to the identified chemical environments of S_1 and S_4 and S_2 and S_3.

(3) In all of the species, the rhombic moieties $M-(\mu\text{-}S_1)-(\mu\text{-}S_4)-M'_1$ and $M-(\mu\text{-}S_2)(\mu\text{-}S_3)-M'_2$ are adjusted. Bond angles $\angle S_1-M-S_4$ and $\angle S_2-M-S_3$ remain comparable to each other, but both are increased, while $\angle S_1-M'_1-S_4$ and $\angle S_2-M'_2-S_3$, also remaining comparable to each other, decreased. Furthermore, though it seems that molecules **I** and **III** are preferable to form a more normal (MS_4) tetrahedron, it is apparently not the case for others.

(43) Stalick, J. K.; Siedle, A. R.; Mighell, A. D.; Hubbard,C. R. *J. Am. Chem. Soc.* **1976**, *101*, 2903.

Table 2. Calculated Selected Optimized Bond Lengths (Å) and Angles (deg) of Model Clusters[a]

atoms	I	II	III	IV	V	VI
			Bond Lengths			
$M-M'_1$	2.895	3.204	2.924	3.247	2.893	2.920
$M-M'_2$	2.750	2.995	2.776	3.024	2.894	2.919
$M-S^b$	2.270	2.268	2.271	2.270	2.285	2.287
M'_1-S^b	2.455	2.723	2.472	2.740	2.573	2.592
M'_2-S^b	2.374	2.614	2.388	2.624	2.573	2.591
M'_1-P^c	2.410	2.628	2.407	2.624	2.427	2.423
M'_2-P	2.327	2.543	2.323	2.540	2.427	2.423
			Bond Angles			
$M'_1-M-M'_2$	180.00	180.00	180.00	179.68	178.39	180.00
S_1-M-S_4	110.50	113.36	110.38	112.65	116.34	116.40
$S_1-M'_1-S_4$	98.16	87.58	97.30	86.56	98.00	97.17
$M-S_1-M'_1$	75.67	79.54	76.16	80.39	73.06	72.93
$M-S_4-M'_1$	75.68	79.52	76.16	80.39	72.60	73.50
S_2-M-S_3	110.71	114.99	110.57	114.49	116.33	116.39
$S_2-M'_2-S_3$	104.49	94.82	103.58	94.06	97.98	97.19
$M-S_2-M'_2$	72.38	75.07	72.90	75.71	73.00	73.42
$M-S_3-M'_2$	72.42	75.11	72.94	75.75	72.67	72.99

[a] Notes: M = Mo for **I**, **II**, and **V** and W for **III**, **IV**, and **VI**; M′ = Cu for **I** and **III**, Ag for **II** and **IV**, and Au for **V** and **VI**. [b] Averaged value. [c] Averaged value for **I**−**IV**.

Table 3. Calculated Results of Dipole Moments (Unit: D) and First-Order Hyperpolarizabilities (Unit: au) of the Six Clusters

	group 1			group 2		
	I	**II**	**III**	**IV**	**V**	**VI**
μ_x	−0.1492	−0.1559	−0.1308	−0.1330	0.0026	0.0019
μ_y	0.0208	0.0241	0.0222	−0.0038	−0.0348	0.0603
μ_z	0.0215	0.0312	0.0176	−0.0233	0.0173	0.0395
β_{xxx}	−579.66	−798.76	−523.74	−753.29	1.83	1.53
β_{yyy}	5.94	6.27	−6.50	8.70	−2.67	5.03
β_{zzz}	−10.86	−7.80	−12.76	5.43	4.42	6.59
$\beta_{x,av}$	−467.36	−705.87	−392.74	−634.14	33.56	−55.54
$\beta_{y,av}$	300.70	297.57	313.08	311.19	94.47	71.79
$\beta_{z,av}$	−88.88	−105.47	−87.82	−96.12	−80.57	−86.78

(4) Comparisons of the structural data between molecules **I** and **III**, **II** and **IV**, and **V** and **VI** show impressive similarities between Mo and W analogues, which is not unusual for the well-known "lanthanide contraction". As for the elements Cu, Ag, and Au, the corresponding bond lengths display a uniform but particular order (Mo(W)−Cu_2 < Mo(W)−Au < Mo(W)−Ag_2; Cu_2-S < Au_1/Au_2-S < Ag_2-S and Cu_2-P < Au−P < Ag_2-P), regardless of the optimized or original structures.

In conclusion, simplification and optimization processes were reasonable, permitting practical implementation of the finite field method on the optimized molecules **I**−**VI**, which are treated as the fine and simple simulating models of prototypes a−f. The affinity between Mo(W) and S was greater than that between Cu (Ag, Au) and S, and the moiety [Mo(W)S_4] was the central bridge in these clusters. The properties of Mo and W analogues are more similar to each other than are those of analogous Cu, Ag, and Au clusters.

Electronic Structures and Linear and Nonlinear Hyperpolarizabilities of Group 1. One of the most striking features of Mo/W−S transition metal cluster compounds is that the building blocks of quadrangular M−(μ-S)$_2$−M′ (M = V, Mo, W; M′ = Fe, Co, etc.) have extensive π-electron delocalization over the four-membered ring.[44] The p orbitals on bridging S atoms largely contribute to frontier molecular orbitals. The M−(μ-S) bond, which was demonstrated as the strongest atom−atom interaction, was the main factor in stabilizing the cluster systems. The selected series of linear-shaped compounds a−f, without exception, have analogous electronic configurations and properties. In this paper, however, we emphasized the electronic field perturbation effects and relationships between molecular NLO properties and microscopic structures.

The selected results of calculated dipole moments and the first-order hyperpolarizabilities are given in Table 3. However, the first-order hyperpolarizabilities will be of less concern. This is because many Mo(W)−S(Se)−Cu(Ag, Au) cluster crystals (including those selected prototypes a−f) are centrosymmetric, and it is the third-order optical nonlinearities that are of greatest interest to us. Moreover, it can be seen from eqs 2 and 4 that it is rather difficult to define the physical meaning of the quantity $\sigma\Delta E(F_i) + \Delta E(-\sigma F_i)$. However, it can also be seen that, to some extent, the magnitude of β_{iii} will roughly follow that of μ_i, the dipole moment in the corresponding direction. In Table 3, models **V** and **VI** of group 2, which are nearly centrosymmetric, have negligible dipole moments and first hyperpolarizabilities, while those of group 1, with negligible μ_y and μ_z but larger μ_x values, have negligible β_{yyy} ($\beta_{y,av}$) and β_z ($\beta_{z,av}$), but more considerable β_{xxx} and hence $\beta_{x,av}$. The difference is impressive. Though the relative order of μ_i will not coincide with that of β_{iii} or $\beta_{i,av}$ due to nonlinearity, it can be expected

(44) For example. Szterenberg, L.; Trazebiatowska, B. J. *Inorg. Chim. Acta* **1984**, *86*, L29.

Table 4. Calculated Results of Linear Polarizabilities (Unit: au) and Second-Order Hyperpolarizabilities (Unit: au) of the Six Model Clusters

	group 1			group 2		
	I	**II**	**III**	**IV**	**V**	**VI**
α_{xx}	342.114	351.160	330.573	341.878	393.979	383.060
α_{yy}	205.633	220.322	203.452	217.669	175.192	173.122
α_{zz}	177.981	187.918	176.214	184.979	175.356	173.182
α_{av}	241.909	253.134	236.747	248.175	248.176	243.121
γ_{xxxx}	325710	469310	292397	426557	409873	393967
γ_{yyyy}	35370	44693	35247	45053	4480	4707
γ_{zzzz}	7643	7613	7343	6947	3953	3717
γ_{xxyy}	43602	55400	40280	52152	5080	6253
γ_{yyzz}	3309	3731	3027	3397	2360	1898
γ_{zzxx}	8411	15003	9570	16208	5258	6322
γ_{av}	95873	133977	88148	124414	88740	86267

Table 5. NBO Charge Populations of Model Clusters **I** and **II**[a]

	$MoS_4Cu(PH_3)_2Cu(PH_3)$ (**I**)			$MoS_4Ag(PH_3)_2Ag(PH_3)$ (**II**)		
	free	$F_x = 0.0050$ au	$F_x = 0.0050$ au	free	$F_x = 0.0050$ au	$F_x = 0.0050$ au
P'_1/P_2	−0.013	0.001	−0.026	−0.008	0.002	−0.018
M'_1	0.709	0.702 (−0.007)	0.716 (0.007)	0.682	0.672 (−0.010)	0.689 (0.007)
S_1/S_4	−0.367	−0.413 (−0.046)	−0.321 (0.046)	−0.364	−0.409 (0.045)	−0.318 (0.046)
M	−0.124	−0.126	−0.122	−0.099	−0.102	−0.098
M'_2	0.704	0.715 (0.011)	0.691 (−0.013)	0.666	0.678 (0.012)	0.647 (−0.019)
S_2/S_3	−0.404	−0.359 (0.045)	−0.445 (−0.0 41)	−0.399	−0.355 (0.044)	−0.440 (−0.041)
P_3	−0.012	−0.033	0.010	−0.009	−0.030	0.013

[a] Note: The slash between S atoms or P atoms means averaged values.

that much larger first-order hyperpolarizabilities will be obtained by construction of unsymmetrical clusters with larger dipole moments.

On the other hand, as exhibited in eqs 3 and 5, the second-order hyperpolarizablity components γ_{iiii}, as well as those of linear polarizability α_{ii}, are related to the quantities $\Delta E(F_i) + \Delta E(-F_i)$, which are believed to reflect the susceptibility of electronic systems. The absolute values of α_{ii} and γ_{iiii} will be definitely determined by a difference $\{\sigma[\Delta E(F_i) + \Delta E(-F_i)] - [\Delta E(\sigma F_i) + \Delta E(-\sigma F_i)]\}$ or $\sigma[\Delta E(F_i) - \Delta E(\sigma F_i)]$, which relates to the electronic susceptibility of the molecule in the *i* direction. Fortunately, the selected model construction is so clear that it permits us to explore the relations between the external field perturbation effects on the electronic structures and the third-order hyperpolarizabilities in depth. The selected results of calculated linear polarizabilities and the second-order hyperpolarizabilities are given in Table 4.

Models in group 1 have similar structures and, impressively, similar NLO properties. The first one is the anisotropy of molecular NLO properties reported in Table 4. The components with *x* subscripts are much larger than those with only *y* or *z*. In each model cluster, $\gamma_{xxxx} > \gamma_{yyyy} > \gamma_{zzzz}$ ladder with 1 order of magnitude and $\gamma_{xxyy} \gg \gamma_{zzxx} > \gamma_{yyzz}$. Second, the two terminal phosphine ligands coordinated to M'_1 in group 1, though important to γ_{yyyy}, contribute much less to γ_{av} due to the dominance of γ_{xxxx}.

The natural bond orbital (NBO) population in the following three typical cases of models **I** and **II** are listed in Table 5: case 1, free status; case 2, models under the perturbation of $E(F_x = 0.0050, 0, 0)$; case 3, $E(F_x = -0.0050, 0, 0)$. The charge transfers occur solely between the three-atom groups $M'_1(\mu\text{-}S_1,\mu\text{-}S_4)$ and $M'_2(\mu\text{-}S_2,\mu\text{-}S_3)$, from the latter to the former in case 2 and from the former to the latter in case 3. Although only two representatives (models **I** and **II**) were listed in Table 5, the analyzed results for other models have the same conclusions. Collectively, the models of group 1 can be deemed as a combination of two perpendicular fragments separated by one Mo or W center. It is the electric-field-induced charge transfer from one segment to the other that invokes optical nonlinearity. Unlike the great planar electron conjunction systems with alternate charge densities on neighboring atoms common in many organic NLO materials,[45] these thiomolybdate/thiotungstate−sulfur transition metal clusters display an essentially distinct delocalization and transition character. The charge import and export are carried out as a homogeneous ensemble through the thiomolybdate/thiotungstate group. Figuratively, it seems the "electronic clouds" over the two segments will oscillate when a light beam acts on the cluster. The magnitude of electron flow under the perturbation is significant and promising.

Analyses of the frontier orbitals show that, for all species, HOMOs do not alter much while there are remarkable changes on LUMOs. In Figure 3, it is the 3p orbitals of μ-S atoms that contribute mainly to HOMO of the molecules, and the orbital components differ slightly from cases 1 and 2. On the other hand, there are significant deviations on the extensive LUMOs in both cases 2 and 3 from the free status. In group 1, the enhancement of p_x of M'_1 and 2s of P_1 and P_2 contribute most to the deviation in case 1; the 2s orbitals of the three hydrogen atoms bonded to P_3, especially 2s of P_3, are responsible in case 2. This may indicate electronic fields predominantly affect the excited states of the molecules. In fact, energy gaps are slightly but unanimously decreased under external fields due to the slight decreasing of LOMO eigenvalues. The shapes in Figure 3d are considerably different from those in Figure 3e due to structural asymmetry.

(45) Messier, J.; Kajar, F.; Prasad, P. N. Eds. *Organic Molecules for Nonlinear Optics and Photonics*, Kluwer Scientific Publishers: Dordrecht, 1991.

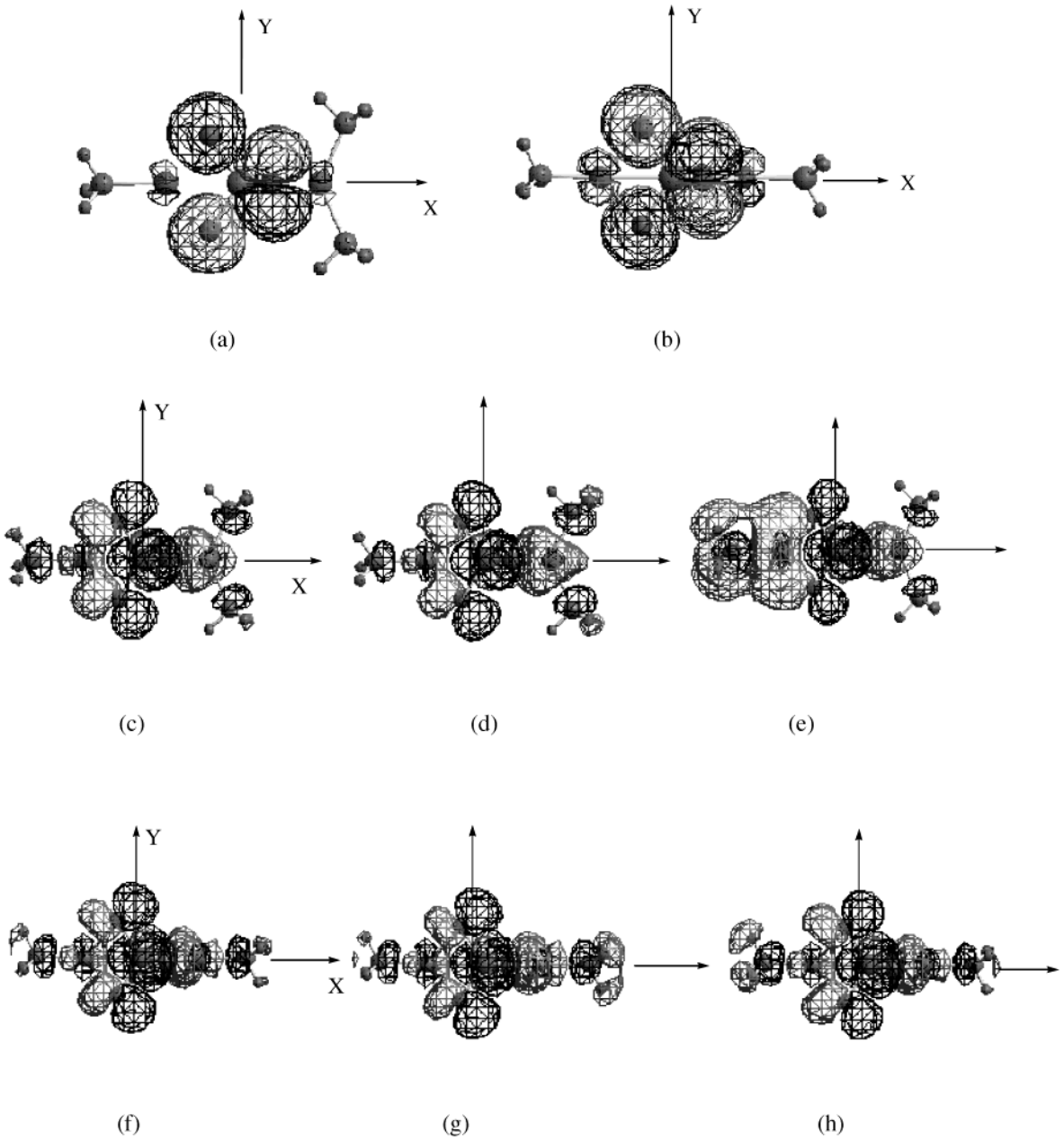

Figure 3. Contour graphs of frontier orbitals (a) HOMO of molecule II, (b) HOMO of molecule V, (c) LUMO of molecule II in free state, (d) LUMO of molecule II with F_x= 0.005 au, (e) LUMO of molecule II with F_x= −0.005 au. (f) LUMO of molecule V in free state, (g) LUMO of molecule V with F_x=0.005 au and (h) LUMO of molecule V with F_x = −0.005 au.

Element Substitution Effects. As have been mentioned, similarities of structural and electronic properties among these series of model molecules are impressive. The close energy gaps (0.105−0.128 au) imply there may be no essential difference in stability either. In a comparison of molecules **I** with **III** and **II** with **IV**, the similar properties such as interatomic distances and bond angles in Table 2, dipole moments and the first-order hyperpolarizabilities in Table 3, calculated linear polarizabilities and the second-order hyperpolarizabilities in Table 4, and NBO net atomic charges in Table 5 satisfactorily coincide. As far as NLO properties are concerned, Mo compounds are a little better than their W counterparts, but the differences are not significant.

Comparison of the properties of copper compounds (**I** and **III**) with silver compounds (**II** and **IV**) shows a general rule that Ag compounds are much better than their Cu counterparts. In Table 5, the amounts of gain or lose of charges on the Ag atoms are slightly larger than those on Cu atoms, while those on S atoms are nearly identical. This fact concurs in agreement with stating that Ag is much softer than Cu. The fragments M−(μ-S)$_2$−M′ will possess a more extensive and intensive electronic delocalization when M′ = Ag than M′ = Cu.

Second-Order Hyperpolarizabilities of Model Clusters of Group 2. Models **V** and **VI** in group 2 have two nearly identical moieties M(μ-S)$_2$Au (M = Mo, W) perpendicular to each other. The two sides of the central M atoms are

chemically indistinguishable, but the sulfur-bridged metal cores again are the main source of NLO response. Therefore, in the group 2 (Table 4) the orders are as follows: $\gamma_{xxxx} \gg \gamma_{yyyy} \sim \gamma_{zzzz}$ and $\gamma_{xxyy} \sim \gamma_{zzxx} > \gamma_{yyzz}$ ($\gg$ means larger than 2 orders of magnitude and $\sim$ means comparable).

Analyses of the frontier orbitals show that HOMOs do not alter much. In Figure 3b, it is the p orbitals of μ-S atoms that contribute mainly to HOMO of the molecules. This is very similar to the cases of group 1. On the other hand, Figure 3f−h shows there are significant deviations among the extensive LOMOs in cases 2 and 3 from the free status in a similar way to that in group 1. However, the actual symmetry on two sides of M determines the symmetric shapes of LUMOs in cases 2 and 3.

The small first-order hyperpolarizabilities of gold compounds **V** and **VI** are due to symmetric structures. Element substitution effect can be seen as less important. First, in the case of the second-order hyperpolarizabilities, the Mo/W element substitution effect of model clusters in the group 2 is analogous to that in group 1. Again, the NLO properties of the Mo compound (model **V**) are a little better than their W counterparts (model **VI**). Second, γ_{xxxx}(Au) values are smaller than γ_{xxxx}(Ag) but larger than γ_{xxxx}(Cu). From the NBO analysis the electron delocalization of Au compounds is the largest. But charges on Au are the most negative and the degree of charge transfer the smallest, indicating the Au atom is "harder" than Cu and Ag. When compared with Ag systems, this effect is somewhat greater than the delocalization effect, while, with Cu compounds, it is the other way around.

Concluding Remarks

We present, in this work, DFT calculations of NLO properties of a series of trinuclear-cored Mo(W)−S−Cu-(Ag, Au) cluster compounds. The compounds are simplified and geometrically optimized to form model clusters. The simplification and optimization are justifiable. A scheme of finite field approach was applied to compute the molecular NLO properties of the models. The results revealed the relationships between optical nonlinearity and geometric and electronic structures.

Several conclusions can be drawn from the study. The model molecules, although they can be divided into two subgroups, are alike in the structure of two fragments of rhombic units M−(μ-S)$_2$−M′ (M = Mo, W; M′ = Cu, Ag, Au), perpendicular to each other, which are joined by sharing the bridge metal atom M. It is the charge transfers from one of these moieties to the other in these characteristic sulfido−transition metal cores that are responsible for polarizabilities and hyperpolarizabilities. This kind of electronic delocalization, differentiated from that of a planar π-system, is interesting and worthy of further investigations. The structural effects on properties are important. In subgroup 1, considerable second-order nonlinearities are exhibited. The element substitution effect of Mo and W is weak, while that of Cu and Ag is considerable. For convenience, an overall order can be written as the following: γ_{xxxx}(Mo−Ag) > γ_{xxxx}(W−Ag) > γ_{xxxx}(Mo−Au) > γ_{xxxx}-(W−Au) > γ_{xxxx}(Mo−Cu) > γ_{xxxx}(W−Cu) and γ_{av} (Mo−Ag) $\sim$ γ_{av}(W−Ag) > γ_{av}(Mo−Au) $\sim$ γ_{av}(W−Au) $\sim$ γ_{av}(Mo−Cu) $\sim$ γ_{av}(W−Cu).

Acknowledgment. We acknowledge the National Science Foundation of China (NSFC, Grants 69978021 and 20173064) and FPNSFC (Grant E9910030) for financial support.

IC025649E